ISSN 1070-3284, Russian Journal of Coordination Chemistry, 2021, Vol. 47, No. 3, pp. 209–218. © Pleiades Publishing, Ltd., 2021.
Russian Text © The Author(s), 2021, published in Koordinatsionnaya Khimiya, 2021, Vol. 47, No. 3, pp. 182–190.

Synthesis and Characterization of the New Cluster Complex $\{Mo_3S_4\}$ with the Hemilabile Phosphine-Selenoether Ligand

N. Yu. Shmelev[a, b], M. I. Gongola[a, b], S. F. Malysheva[c], N. A. Belogorlova[c], A. V. Artem'ev[a], Ya. S. Fomenko[a], V. Yu. Komarov[a, b], K. V. Sopov[b], N. B. Kompan'kov[a], D. G. Sheven'[a], M. N. Sokolov[a, b, d], and A. L. Gushchin[a, *]

[a] *Nikolaev Institute of Inorganic Chemistry, Siberian Branch, Russian Academy of Sciences, Novosibirsk, Russia*

[b] *Novosibirsk State University, Novosibirsk, Russia*

[c] *Favorsky Institute of Chemistry, Siberian Branch, Russian Academy of Sciences, Irkutsk, Russia*

[d] *Butlerov Institute of Chemistry, Kazan Federal University, Kazan, Russia*

**e-mail: gushchin@niic.nsc.ru*

Received September 3, 2020; revised September 30, 2020; accepted October 6, 2020

Abstract—The reaction of $[Mo_3S_4(Tu)_8(H_2O)]Cl_4{\cdot}4H_2O$ (Tu is thiourea) with $(PhCH_2CH_2)_2PCH_2CH_2SeC_5H_{11}$) (PSe) followed by purification on a chromatographic column packed with silica gel using a saturated solution of KPF_6 in acetone as an eluent results in the formation of $[Mo_3S_4Cl_3(PSe)_3]PF_6$ (**I**) in a yield of 44%. Compound **I** is characterized by X-ray diffraction analysis, ^1H, $^{31}P\{^1H\}$, and ^{77}Se NMR spectroscopy, IR spectroscopy, UV-Vis spectroscopy, cyclic voltammetry, and electrospray ionization mass spectrometry. Several species differed in the coordination mode of three PSe ligands, which can bind to molybdenum via one (phosphorus) or two (phosphorus and selenium) donor atoms, are formed in a solution of compound **I** at room temperature. This behavior is not observed for the compounds similar in structure with PS ligands of an analogous type. Complex **I** demonstrates a higher catalytic activity than its analogue with the PS ligand in the reduction of nitrobenzene to aniline under the action of diphenylsilane.

Keywords: clusters, molybdenum, hemilabile ligands, phosphine-chalcoethers, synthesis, crystal structure, catalytic properties

DOI: 10.1134/S1070328421030040

INTRODUCTION

Hemilabile ligands play an important role in coordination chemistry and metal complex catalysis. The key feature of these polydentate ligands is the presence of several types of donor atoms with different affinities to a specific metal center, which favors the formation of coordinatively unsaturated metal centers via the reversible cleavage of the metal–ligand bond with a weaker donor atom during the catalytic cycle [1]. The controlled coordination–decoordination of the labile donating function of the hemilabile ligand can also be used for the activation of small molecules [2–13].

The reactivity of the hemilabile ligands in the mononuclear compounds was studied in rather detail. The polynuclear and cluster compounds with hemilabile ligands remain fairly poorly studied [14–19]. However, in the last case, the hemilabile ligand can perform several functions: chelating, bridging, or monodentate. The existence of the kinetically favorable products with the bridging functions and thermodynamically favorable products with the chelating function of the hemilabile ligands was shown for the well studied trinuclear carbonyl clusters of osmium and ruthenium with the thioether ligands [20–24].

The systematic studies in the area of trinuclear clusters of molybdenum and tungsten with chalogenide bridges were carried out at the Nikolaev Institute of Inorganic Chemistry (Siberian Branch of the Russian Academy of Sciences) [25–36]. The recent studies of the $\{M_3S_4\}$ derivatives (M = Mo, W) with the *N*,*N*'-chelating ligands, such as 2,2'-bipyridine, 1,10-phenanthroline, and their analogues [37–45], showed prospects of using these compounds in homogeneous catalysis [41, 46–49], for the activation of acetylenes [50], and in bioinorganic chemistry [45].

The bifunctional phosphine-thioethers (PS) with different functional groups for coordination to the clusters $\{M_3S_4\}$ (M = Mo, W) were used in our recent works [51, 52]. As a result, we obtained the cationic complexes $[M_3S_4Cl_3(PS)_3]^+$ in which all the three PS ligands coordinated to the metal via the bidentate mode. These cationic complexes are capable of transforming into neutral complexes $[M_3S_4Cl_4(PS)_2(PS^*)]$ in which one of the bidentate PS ligands becomes

P-monodentate (PS*) in the presence of chloride ions. The equilibrium constants of these reactions estimated from the data of NMR spectroscopy can serve as a quantitative characteristic of the hemilabile behavior of these ligands, which is more pronounced in the case of Mo_3S_4 compared to W_3S_4. Less donating substituents (aryl instead of alkyl) at the sulfur atom of the PS ligands also favors an increase in the hemilabile properties due to a decrease in the donor ability of sulfur. The enhanced lability of the M–S bond should increase the catalytic activity due to the formation of a coordination vacancy. Indeed, according to this tendency, the $[Mo_3S_4Cl_3(PS1)_3]^+$ complex with the phenyl substituent at the sulfur atom exhibits a high catalytic activity in the reduction of nitrobenzene to aniline under the action of Ph_2SiH_2 [52]. The tungsten complexes are characterized by a much lower catalytic activity in this process [51].

Extending the studies in this area, here we report the synthesis of a new cluster molybdenum complex with the phosphine-selenoether ligand and the influence of the nature of the chalcogen donor atom on the hemilabile and catalytic properties.

EXPERIMENTAL

Experiments on the synthesis of compound $[Mo_3S_4Cl_3(PSe)_3]PF_6$ (**I**) were carried out using an argon–vacuum line. The starting compounds $[Mo_3S_4(Tu)_8(H_2O)]Cl_4{\cdot}4H_2O$ and phosphine-selenoether (bis(2-phenylethyl)[2-(pentylselenyl)ethyl]-phosphine, PSe) were synthesized according to published procedures [53, 54]. Potassium hexafluorophosphate (KPF_6) was received from commercial sources and used without additional purification.

Elemental C,H,N analyses were carried out on a EuroEA3000 Eurovector analyzer. IR spectra (4000–400 cm^{-1}) were recorded on a Perkin-Elmer System 2000 FTIR spectrophotometer for samples in KBr pellets. ^1H, $^{31}P\{^1H\}$, and ^{77}Se NMR spectra were measured at room temperature in CD_3CN and CD_2Cl_2 solutions in 5-mm tubes on a Bruker Avance 500 spectrometer with frequencies of 500 (^1H), 202.46 (^{31}P), and 113.63 (^{77}Se) MHz. Chemical shifts were assigned using TMS (^1H), 85% H_3PO_4 (^{31}P), and ^{77}Se ($(CH_3)_2Se$) as standards. UV–Vis spectra were recorded on a Specord M40, Helios γ spectrophotometer in a range of 200–900 nm in a CH_3CN solution. Electrospray ionization mass spectrometry was carried out on an Agilent, 6130 Quadrupole MS, 1260 infinity LC mass spectrometer. The following conditions were used: voltage on the capillary 2.0 kV, nitrogen as drying gas, 300 L/h, and 120–150°C. The observed isotopic distribution of each component was well consistent with the theoretical distribution calculated using the MassLynx 4.1 program.

Cyclic voltammograms were detected on a 797 VA Computrance electrochemical analyzer (Metrohm, Switzerland). All measurements were carried out in a three-electrode cell consisting of a working glassy carbon electrode, a platinum auxiliary electrode, and a silver chloride (Ag/AgCl) reference electrode filled with a solution of KCl (c = 3 mol/L). The solvent (CH_3CN) was degassed by purging argon for 1–2 min prior to every recording. A solution of Bu_4NPF_6 (c = 0.1 mol/L) was used as an electrolyte. The concentration of the studied complex was ~1×10^{-1} mol/L. The potentials ($E_{1/2}$) were determined as $1/2(E_a + E_c)$, where E_a and E_c were the anodic and cathodic potentials, respectively.

Thermogravimetric analysis (TG) was carried out on a TG 209 F1 Iris thermobalance (NETZSCH) in an inert atmosphere (He).

Synthesis of $[Mo_3S_4Cl_3(PSe)_3]PF_6$ (I). A mixture of $[Mo_3S_4(Tu)_8(H_2O)]Cl_4{\cdot}4H_2O$ (0.40 g, 0.32 mmol), PSe (0.61 g, 1.1 mmol), and CH_3CN (40 mL) was stirred on reflux for 5 h. After cooling to room temperature, the reaction mixture was evaporated to dryness, and CH_2Cl_2 was added to the solid residue. An insoluble precipitate of thiourea was separated by filtration. The filtrate was deposited on a chromatographic column packed with silica gel (Sigma Aldrich, pore size 60 Å), washed with CH_2Cl_2, and eluted with a solution of KPF_6 in acetone (10 mg/mL). The resulting solution was evaporated to dryness, CH_2Cl_2 was added to the solid residue, and an undissolved precipitate of inorganic salts was filtered off. *n*-Hexane excess was layered on the solution. As a result, a green crystalline product of **I**·2.5CH2Cl2 was obtained. The yield was 0.273 g (44%). TG: the mass loss (3.87%) in the range from room temperature to 205°C corresponded to the removal of one solvate molecule of dichloromethane.

For $C_{69}H_{99}F_6P_4S_4Cl_3Se_3Mo_3{\cdot}2.5CH_2Cl_2$		
Anal. calcd., %	H, 4.9	C, 40.2
Found, %	H, 4.8	C, 40.1

IR (ν, cm^{-1}): 3359 m, 3194 m, 3060 m, 3025 m, 2954 m, 2927 m, 2857 m, 2044 w, 1624 m, 1603 m, 1496 m, 1454 s, 1407 m, 1288 m, 1208 m, 1137 m, 1029 w, 998 m, 957 w, 839 s, 739 s, 698 s, 557 s, 495 m, 432 m.

$^{31}P\{^1H\}$ NMR (CD_3CN, 25°C), δ, ppm: 42.25 s, 42.08 s, 41.58 s, 41.45 s, 41.26 s, 41.19 s, –144.6 (sept.). $^{31}P\{^1H\}$ NMR (CD_2Cl_2, 25°C) δ, ppm: 40.2 s, 40.1 s, 39.9 s, 39.7 s, 39.4 s, 39.2 s, –144.4 (sept.). ^1H NMR (CD_3CN), δ, ppm: 6.67–7.44 (m, 30H, Ph); 2.74–2.87 (m, 12H, C$\underline{H}_2$Ph); 2.40–2.50 (m, 6H, SeC$\underline{H}_2$CH$_2$P); 2.20 (m, 6H, SeC$\underline{H}_2$Bu); 1.68–1.85 (m, 18H, C$\underline{H}_2$PC$\underline{H}_2$); 1.54 (m, 6H, C$\underline{H}_2$Pr); 1.33–1.40 (m, 12H, (C$\underline{H}_2$)$_2$Me); 0.92 (m, 9H, C$\underline{H}_3$). ^{77}Se

Table 1. Crystallographic parameters and structure refinement details for compound **I**

Parameter	Value
FW	2137.96
T, K	100(2)
Space group	$P2_1/n$
a, Å	15.0505(11)
b, Å	24.2362(18)
c, Å	24.6111(16)
β, deg	105.547(3)
V, Å^3	8648.8(11)
Z	4
ρ_{calc}, g/cm^3	1.642
μ, mm^{-1}	2.161
Crystal size, mm	0.447 × 0.36 × 0.15
Range of 2θ, deg	2.4–51.4
Number of measured/independent reflections	46636/15875
$R_{int}/R\sigma$	0.0634/0.0910
Number of refined parameters/restraints	702/213
GOOF	1.062
R_1/wR_2 for $I \geq 2\sigma(I)$	0.1484/0.3095
R_1/wR_2 for all data	0.2179/0.3511
Residual electron density (min/max), e Å^{-3}	−1.56/2.20

NMR (CD_3CN), δ, ppm: 309.7 s, 308.8 s, 267.4 s, 266.6 s, 264.2 s, 263.7 s.

ESI-MSI (+, CH_3CN, *m/z*): 1781.9 ($[Mo_3S_4Cl_3(PSe)_3]^+$).

UV/Vis (CH_3CN), λ, nm (ε, L mol^{-1} cm^{-1}): 251 (14153), 356 (7274), 633 (413).

Catalytic tests. Nitrobenzene (10 μL, 0.097 mmol) and Ph_2SiH_2 (3.5 equiv) were added to a preliminarily deaerated solution of compound **I** (9.66 mg, 0.0050 mmol) in a CH_3CN–CD_3CN mixture (V_{CH_3CN} : V_{CD_3CN} = 3 : 1, 2 mL). The reaction mixture was stirred at room temperature for 16 h. Aliquots taken from the final and initial solutions before the addition of Ph_2SiH_2 were analyzed by ^{1}H NMR spectroscopy. No conversion of nitrobenzene was observed before Ph_2SiH_2 was added. After the end of the reaction, the conversion of nitrobenzene was 87%. The yield of compound **I** was 48%.

X-ray diffraction analysis (XRD). A single crystal of compound **I** was taken from the mother liquor and rapidly cooled to 100 K in a jet of an N_2 cryostat. The XRD data were obtained on a Bruker APEX Duo automated four-circle diffractometer with a two-coordinate CCD detector (MoK_α, λ = 0.71073 Å, graphite monochromator) in the ω scan mode with an exposure of 240 s/deg. Integration was performed and an absorption correction was applied by equivalent reflection intensities using the APEX2 program package [55]. The structure was solved using the SHELXT program [56] and refined using Olex2 [57] implemented in SHELXL [56]. The main crystallographic data and structure refinement details are presented in Table 1. The positions of the non-hydrogen atoms of the cluster cation and PF_6^- anion were obtained by searching for the primary model or from the difference synthesis and refined in the anisotropic approximation. Hydrocarbon fragments with carbon atoms with high anisotropy of atomic displacements or having significant residual electron density peaks were refined as those split into two conformations with restraints imposed on the bond and angular distances. The atomic displacement parameters for closely arranged carbon atoms from alternative conformations were accepted to be equal or were fixed. Hydrogen atoms were specified geometrically and refined by the riding model. Six highest peaks of the residual electron density (2.2–1.2 e/Å^3) were localized near the Mo and Se atoms (see Discussion). The nonlocalized electron density in the cavities between the ions was taken into account using the Solvent Mask procedure of the Olex2 program.

The coordinates of atoms and thermal parameters were deposited with the Cambridge Crystallographic

Data Centre (CIF file CCDC no. 2016802; https://www.ccdc.cam.ac.uk/structures/).

RESULTS AND DISCUSSION

The $[M_3S_4(Tu)_8(H_2O)]^{4+}$ complexes (M = Mo, W) containing coordinated thiourea (Tu) molecules were shown to be very labile and readily react in ligand exchange reactions with the formation of diverse derivatives $\{M_3S_4\}$ [40, 50–52]. For example, the reactions of $[M_3S_4(Tu)_8(H_2O)]^{4+}$ with phosphine-thioethers PS1 and PS2, whose structures are shown in Scheme 1, afford complexes $[M_3S_4Cl_3(PS)_3]^+$ in which each metal atom is bonded to the PS ligand via the bidentate mode.

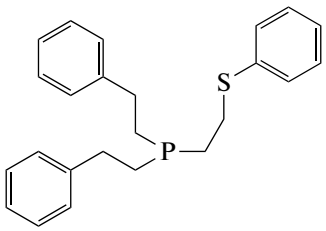

PS1

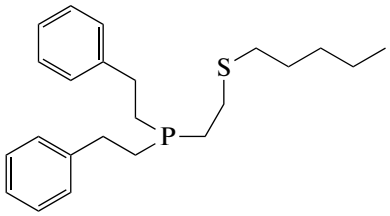

PS2

Scheme 1.

One of important tasks of this work was to reveal distinctions in the properties of the cluster compounds upon the substitution of sulfur by selenium in the ligand structure. Phosphine-selenoether (PSe) presented in Scheme 1 was used for this purpose. It was assumed that the presence of a weaker donor center (selenium instead of sulfur) can result in more pronounced hemilabile properties.

Appling the above described synthetic approach, we synthesized the new complex $[Mo_3S_4Cl_3(PSe)_3]PF_6$ (**I**) in a yield of 44% after purification on a chromatographic column packed with silica gel and recrystallization from a dichloromethane–hexane mixture ($V_{dichloromethane}$: $V_{hexane} \approx 1 : 5$, Scheme 2). A moderate yield of the product can be explained by the sensitivity of the initial phosphine to oxidation and inevitable losses during chromatographic purification and recrystallization.

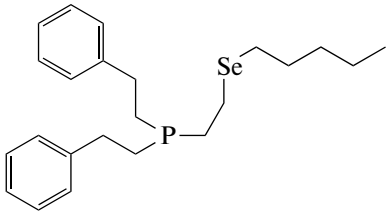

PSe

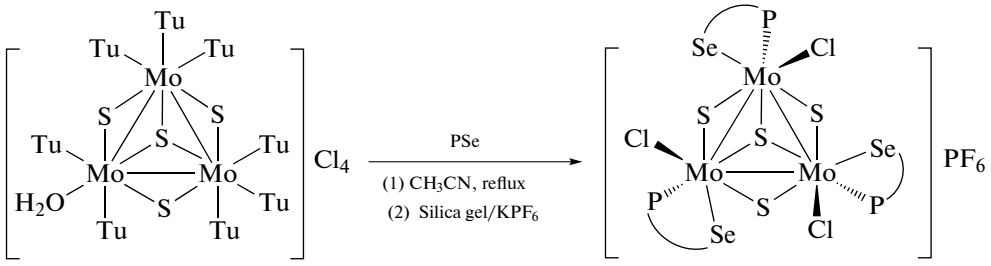

Scheme 2.

Note that complex **I** is a rare example of coordination compounds containing the phosphine-selenoether ligand. A series of works on the complexes of d^8 metals (Ni, Pd, and Pt) containing the phosphine-selenoether ligands was published [58–61].

Single crystals of compound **I** were obtained due to the slow diffusion of hexane to a dichloromethane solution. The structure of the cluster cation $[Mo_3S_4Cl_3(PSe)_3]^+$ is presented in Fig. 1.

Selected bond lengths are presented in Table 2. The molybdenum and sulfur atoms are arranged in such a

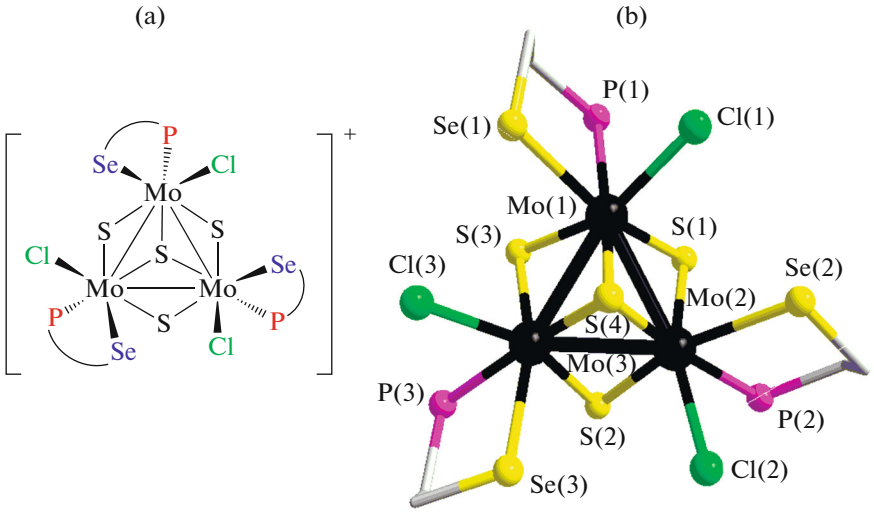

Fig. 1. (a) Simplified structural formula of the cluster cation $[Mo_3S_4Cl_3(PSe)_3]^+$ and (b) the spatial structure of $[Mo_3S_4Cl_3(PSe)_3]^+$ in compound **I**. The substituents at the phosphorus atoms and hydrogen atoms are omitted.

way that the structure of a cube without one vertex, which is typical of compounds of this class, would be formed. The Mo–Mo and Mo–S distances and other geometric parameters are consistent with the published data for the $\{Mo_3S_4\}$ complexes [62–64]. Each molybdenum atom has a distorted octahedral environment consisting of three bridging sulfur atoms, chlorine atom, and phosphorus and selenium atoms of the PSe ligand. All phosphorus atoms are arranged in the *trans* position toward the μ_3-S atom. This spatial arrangement of the heterobidentate ligand is also observed in the $\{M_3S_4\}$ complexes with phosphine-thioethers [52] and aminophosphines [65, 66]. A fairly long distance Mo–Se (2.72–2.74 Å) compared to the usual length of the Mo–Se bond (2.40–2.50 Å) between the metal and chalcogenide ligand of the cluster core of the $\{Mo_3Se_4\}$ [34, 67] and $\{Mo_3Se_7\}$ [33, 44, 68–70] complexes is noteworthy. This explains an easier cleavage of the Mo–Se bond and the possibility of several species to exist in the solution (see below). The presence of the residual electron density near the heavy atoms (Mo, Se) indicates in favor of additional (~5%) modes of arrangement of cations (possibly, isomeric) in the crystal structure of compound **I**. The anomalously high (for 100 K) atomic displacement parameters of all atoms and high anisotropy of the ellipsoids or explicit splittings of the carbon atom positions are related, most likely, to the high conformational mobility of the organic ligands and to the strong disordering of the solvate molecules.

In the crystal structure, the cluster cations and anions PF_6^- form layers perpendicular to the (1 0 −1) direction (diagonally to the vectors *a* and *c* of the lattice, Fig. 2). The layer has cavities of a small volume (~30 Å^3) insufficient for the arrangement of the solvate molecules CH_2Cl_2 or C_6H_{14}. However, the cavities of 524 Å^3 (two cavities per unit cell, 1/2 cavity per formula unit) are observed between the layers, and this volume is sufficient for the incorporation of 3–6 CH_2Cl_2 molecules. The estimation of the electron density as 228 e per cavity obtained using the Olex2 Solvent Mask procedure gives a content of solvate molecules of 2.7 CH_2Cl_2 per formula unit.

The IR spectrum of compound **I** exhibits stretching vibration bands of the C–H bonds at 2857–3060 cm^{-1} and stretching vibration bands of the aromatic rings in a range of 1603–1624 cm^{-1}. The bending vibrations of CH_2 and CH_2P are observed in a range of 1407–1496 cm^{-1}. The characteristic band of vibrations of the Mo_3–μ_3-S fragment is observed at 432 cm^{-1}. The strong absorption bands at 557 and 839 cm^{-1} are assigned to the P–F vibrations of the anion PF_6^-.

The electrospray ionization mass spectrum (ESI-MS) of compound **I** in CH_3CN shows a peak at m/z = 1781.9 with the characteristic isotopic distribution for $[Mo_3S_4Cl_3(PSe)_3]^+$. The UV-Vis spectrum exhibits a

Table 2. Selected bond lengths (Å) in the structure of compound **I**

Bond	*d*, Å
Mo–Mo	2.755(3), 2.762(2), 2.759(2)
Mo–μ_2S	2.304(5), 2.296(4), 2.326(5), 2.308(5), 2.303(8), 2.279(5)
Mo–μ_3S	2.338(6), 2.321(7), 2.344(6)
Mo–Cl	2.453(4), 2.442(6), 2.437(8)
Mo–P	2.544(5), 2.542(7), 2.546(5)
Mo–Se	2.738(3), 2.722(2), 2.738(3)

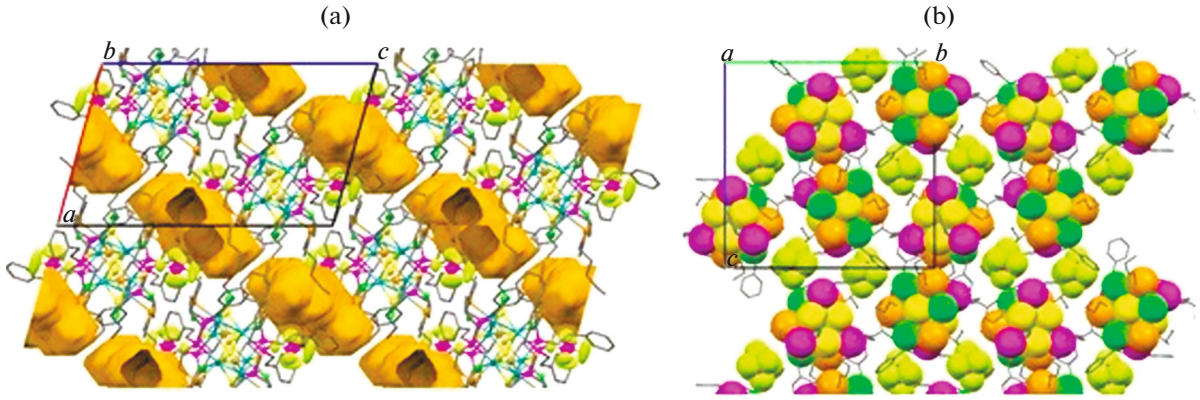

Fig. 2. (a) Projection of the crystal structure of compound **I** along the *b* axis. The cavities accessible for the incorporation of solvate molecules are shown by orange. (b) Projection of the layer perpendicular to the (1 0 −1) direction along the *a* axis. The noncarbon atoms are shown in the van der Waals spheres, and hydrogen atoms are omitted.

weak band at 633 nm (ε = 413 L mol^{-1} cm^{-1}) characteristic of the cluster core $\{Mo_3S_4\}$ [71].

The cyclic voltammogram of compound **I** in CH_3CN demonstrates several consecutive reduction processes characteristic of the $\{Mo_3S_4\}$ cluster core. The first process at −0.49 V (versus Ag/AgCl) is reversible ($\Delta E \approx 80$ mV), which agrees with the data for $[Mo_3S_4Cl_3(PS1)_3]PF_6$ ($E_{1/2}$ = 0.44 V, ΔE = 80 mV) [52]. Other reduction processes at −1.27 and −1.52 V are completely irreversible.

An unusual pattern is observed in the $^{31}P\{^1H\}$ NMR spectrum. Three pairs of signals with close chemical shifts inside each pair are observed instead of one signal as in the spectra of $[M_3S_4Cl_3(PS)_3]^+$ with phosphine-thioethers. At room temperature in CD_3CN, the chemical shifts are 42.25 and 42.08, 41.58 and 41.55, and 41.26 and 41.19 ppm. This correlates with the data of the ^{77}Se NMR spectrum, which also contains three groups of signals: 309.7 and 308.8, 267.4 and 266.6, and 264.2 and 263.7 ppm. This behavior can be explained by the presence in a solution of several species with different coordination modes of the PSe ligand. In the initial compound, all the three PSe ligands are chelating and bonded to molybdenum via both phosphorus and selenium donor atoms. This form exists in the crystal. We assume that one of the ends of the chelate cycle (namely, the end linked with molybdenum via selenium, which is a weaker donor center) is detached in a solution. In this case, the PSe ligand becomes monodentate and bonded to the metal only via the phosphorus atom. Since the complex contains three PSe ligands, the following species can be formed in the solution: with one, two, or three monodentate PSe. The liberated coordination site can be occupied by the solvent molecule L (Fig. 3).

This situation is unique, since the earlier synthesized molybdenum and tungsten complexes $[M_3S_4Cl_3(PS)_3]^+$ with the PS ligands are stable in the solution and the NMR spectra always exhibit only one signal in the characteristic range [51, 52]. The hemilabile properties begin to manifest themselves only upon the reaction of $[M_3S_4Cl_3(PS)_3]^+$ with Cl^-. As a result, one of the Mo–S_L bonds is cleaved, the chloride ion is coordinated, and the neutral complex $[Mo_3S_4Cl_4(PS)_2(PS^*)]$ is formed. The equilibrium constants of these processes were estimated by the $^{31}P\{^1H\}$ NMR method. Interestingly, in the case of tungsten, the formation of a neutral species almost cannot be detected by NMR; i.e., the concentrations of $[W_3S_4Cl_4(PS)_2(PS^*)]$ are very low.

$$\left[Mo_3S_4Cl_3(PS)_3\right]^+ + Cl^- \rightleftarrows \left[Mo_3S_4Cl_4(PS)_2(PS^*)\right]. \quad (1)$$

The $^{31}P\{^1H\}$ NMR spectra of compound **I** in CD_3CN were recorded at various temperatures: −25, −15, 0, 25, 40, and 55°C (Fig. 4). The corresponding chemical shifts (δ_P) of the observed signals are presented in Table 3. Three pairs of the signals can be distinguished at room temperature: with δ_P = 42.25 and 42.08 (I group), 41.58 and 41.45 (II group), and 41.26 and 41.19 ppm (III group). All signals undergo a downfield shift with the temperature increase, and the difference between the chemical shifts of signals in each group decreases. At −25°C, the signals in I and II groups flow together and appear as broadened singlets (42.38 and 41.64 ppm, respectively). The difference between the chemical shifts of the signals of II group was only 0.04 ppm (0.13 ppm at 25°C). An opposite effect is observed with the temperature increase: all signals undergo upfield shifts and become broader, and the difference between the chemical shifts of the signals in each group increases. At 55°C, the signals of III group flow together to form one broad line (41.00 ppm). The pattern observed in the NMR spectra is very complicated, and we cannot interpret it unambiguously at the moment. It can be assumed that

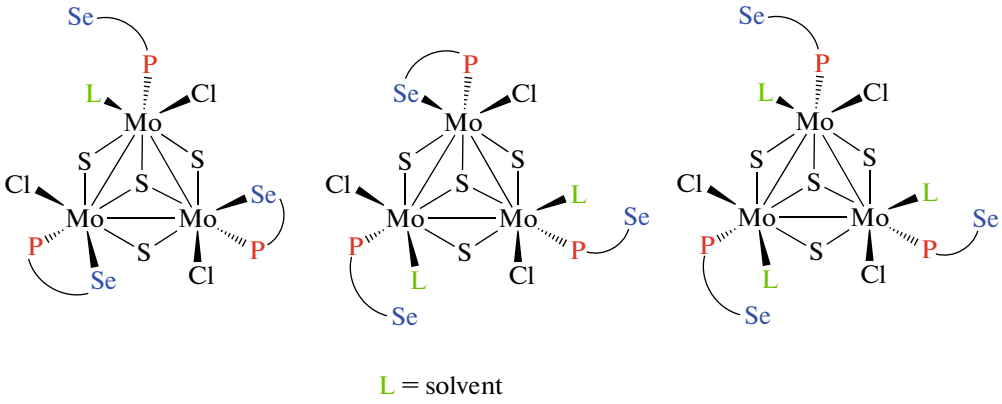

Fig. 3. Schematic representation of different cluster species in the solution.

several parallel processes can occur in a solution of compound **I**. First, as mentioned above, the dissociation of one or several phosphine-selenoether ligands with the Mo–Se bond cleavage to form the structures shown in Fig. 3 is most probable. Second, exchange processes are possible during which selenium and chlorine and/or solvent and chlorine would change their positions, which is favored by chelate ring opening.

It has previously been found that the $\{Mo_3S_4\}$ clusters in various coordination environments are highly active in the catalytic transformation of nitroarenes into the corresponding anilines [47, 48]. Similar tungsten clusters are substantially less active [51]. In this work, complex **I** was tested in the model reaction of nitrobenzene reduction using Ph_2SiH_2 in acetonitrile under mild conditions (room temperature, atmospheric pressure). This reaction was monitored by ^1H NMR spectroscopy using the elaborated procedure [52]. In this case, the conversion of nitrobenzene was 87%, and the yield of aniline was 48%. The obtained values are appreciably higher than those for the $[Mo_3S_4Cl_3(PS2)_3]PF_6$ complex with the same hydrocarbon substituent at the sulfur atom (the conversion is 79%, and the yield of the product is 33%) but are lower than those for $[Mo_3S_4Cl_3(PS1)_3]PF_6$ with the phenyl substituent (conversion 99%, yield 83%). Thus, the replacement of sulfur by selenium in the starting phosphine-chalcoether results in an increase in the catalytic activity of the complex, which can be attributed to more pronounced hemilabile properties of the phosphine-chalcoether ligands in $[Mo_3S_4Cl_3(PSe)_3]PF_6$ compared to $[Mo_3S_4Cl_3(PS2)_3]PF_6$. It can be expected that the replacement of the electron-donating pentyl substituent by the electron-withdrawing phenyl substituent at the selenium atom would lead to a significant increase in the activity, which possibly even exceeds that for $[Mo_3S_4Cl_3(PS1)_3]PF_6$.

Thus, the new trinuclear sulfide cluster complex $[Mo_3S_4Cl_3(PSe)_3]PF_6$ with the phosphine-selenoether ligand was synthesized. The synthesized compound was characterized by the complex of physicochemical methods, including structure determination by single-crystal XRD. Several species differed in the coordination modes of the phosphine-selenoether ligands are formed in the solution of this compound at

Table 3. $^{31}P\{^1H\}$ NMR spectra of compound **I** in CD_3CN at various temperatures

Temperature, °C	Chemical shifts, ppm*
–25	42.38 (I gr.); 41.79, 41.75 (II gr.); 41.64 (III gr.)
–15	42.34, 42.29 (I gr.); 41.71, 41.66 (II gr.); 41.53, 41.51 (III gr.)
0	42.26, 42.15 (I gr.); 41.60, 41.52 (II gr.); 41.37, 41.32 (III gr.)
25	42.25, 42.08 (I gr.); 41.58, 41.45 (II gr.); 41.26, 41.19 (III gr.)
40	42.17, 41.97 (I gr.); 41.49, 41.34 (II gr.); 41.14, 41.06 (III gr.)
55	42.08, 41.87 (I gr.); 41.40, 41.25 (II gr.); 41.00 (III gr.)

* The signals with close chemical shifts (pairs) are assigned to different groups.

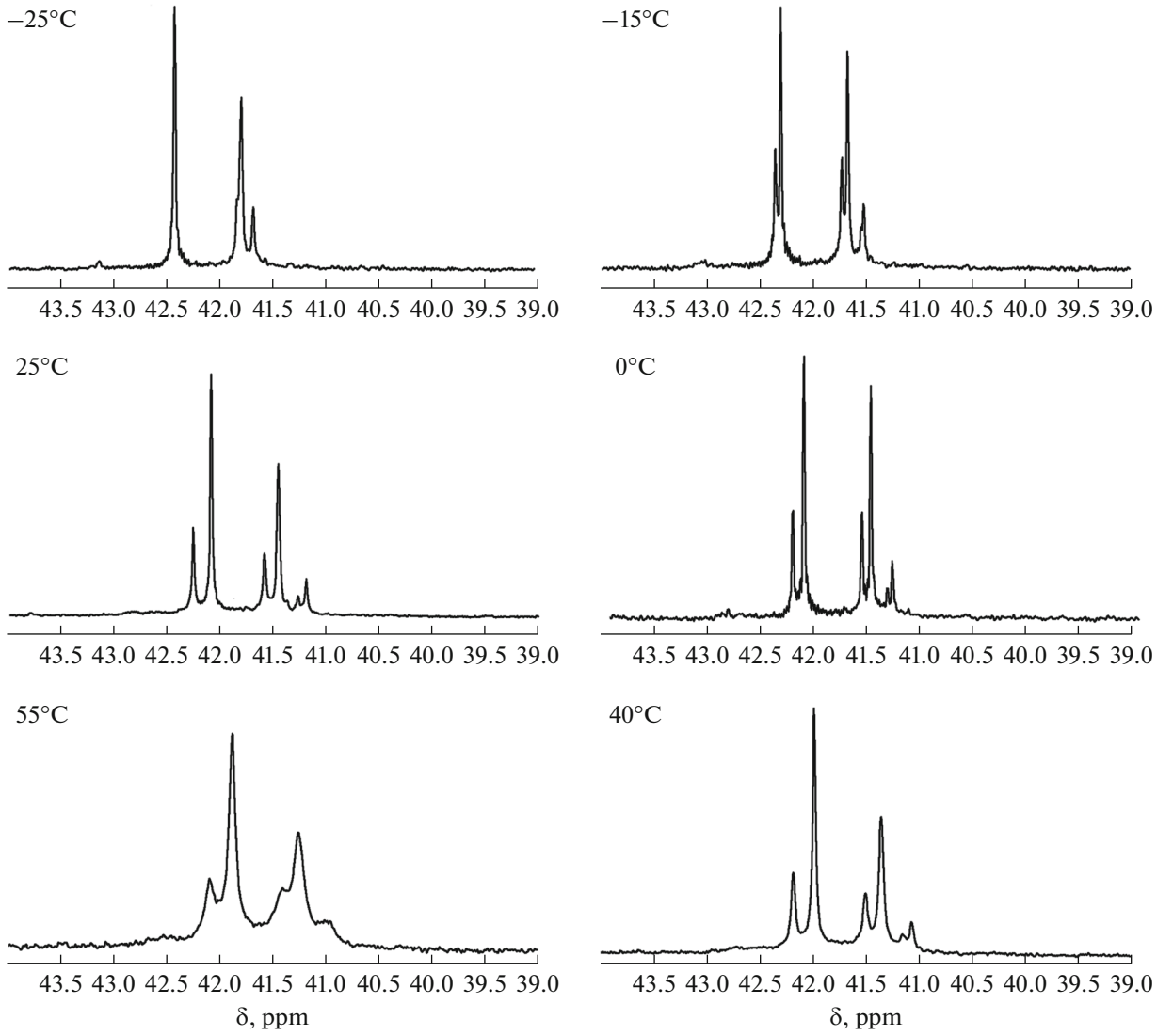

Fig. 4. $^{31}P\{^{1}H\}$ NMR spectra of compound **I** in CD_3CN at various temperatures.

room temperature. The synthesized complex exhibited a higher catalytic activity in the reduction of nitrobenzene to aniline compared to the similar compound containing the phosphine-thioether ligand.

ACKNOWLEDGMENTS

Phosphine-selenoether (PSe) was synthesized in the framework of state assignment no. AAAA-A16-116112510005-7 using the equipment of the Baikal Analytical Center for Collective Use (Siberian Branch of the Russian Academy of Sciences).

FUNDING

This work was supported by the Russian Foundation for Basic Research, projects nos. 18-33-20056 and 19-33-90097.

CONFLICT OF INTEREST

The authors declare that they have no conflicts of interest.

REFERENCES

1. Hor, T.S.A., *Acc. Chem. Res.*, 2007, no. 65, p. 676.
2. Houk, L.W., *J. Organomet. Chem.*, 1980, vol. 192, no. 1, p. C23.
3. Bader, A. and Lindner, E., *Coord. Chem. Rev.*, 1991, vol. 108, no. 1, p. 27.
4. Bierenstiel, M. and Cross, E.D., *Coord. Chem. Rev.*, 2011, vol. 255, nos. 5–6, p. 574.
5. Braunstein, P. and Naud, Â., *Angew. Chem., Int. Ed. Engl.*, 2001, vol. 40, p. 680.
6. Espinet, P. and Soulantica, K., *Coord. Chem. Rev.*, 1999, vols. 193–195, p. 499.

7. Deckers, P.J.W., Hessen, B., and Teuben, J.H., *Angew. Chem., Int. Ed. Engl.*, 2001, vol. 40, no. 13, p. 2516.
8. Ros, A., Estepa, B., Lopez-Rodriguez, R., et al., *Angew. Chem., Int. Ed. Engl.*, 2011, vol. 50, no. 49, p. 11724.
9. Moxham, G.L., Randell-Sly, H.E., Brayshaw, S.K., et al., *Angew. Chem., Int. Ed. Engl.*, 2006, vol. 45, no. 45, p. 7618.
10. Zhang, W.H., Chien, S.W., and Hor, T.S.A., *Coord. Chem. Rev.,* 2011, vol. 255, nos. 17–18, p. 1991.
11. Huynh, H.V., Yeo, C.H., and Chew, Y.X., *Organometallics*, 2010, vol. 29, no. 6, p. 1479.
12. Jiménez, M.V., Pérez-Torrente, J.J., Bartolomé, M.I., et al., *Organometallics*, 2008, vol. 27, no. 2, p. 224.
13. Kuriyama, M., Nagai, K., Yamada, K., et al., *J. Am. Chem. Soc.*, 2002, vol. 124, no. 30, p. 8932.
14. Braunstein, P., Knorr, M., Stern, C., et al., *Coord. Chem. Rev.*, 1998, vol. 180, p. 903.
15. Rasanen, T.M., Jaaskelainen, S., and Pakkanen, T.A., *J. Organomet. Chem.*, 1998, vol. 553, p. 453.
16. King, J.D., Monari, M., and Nordlander, E., *J. Organomet. Chem.*, 1999, vol. 573, p. 272.
17. Deeming, A.J., Shinhmar, M.K., Arce, A.J., et al., *Dalton Trans.*, 1999, vol. 3, p. 1153.
18. Tunik, S.P., Koshevoy, I.O., Poë, A.J., et al., *Dalton Trans.*, 2003, p. 2457.
19. Pakkanen, T.A., *Dalton Trans.*, 2004, vol. 6, p. 2541.
20. Persson, R., Monari, M., Gobetto, R., et al., *Organometallics*, 2001, vol. 20, no. 20, p. 4150.
21. Hrovat, D.A., Nordlander, E., and Richmond, M.G., *Organometallics*, 2012, vol. 31, p. 6608.
22. Persson, R., Stchedroff, M.J., Uebersezig, B., et al., *Organometallics*, 2010, vol. 29, no. 10, p. 2223.
23. Persson, R., Stchedroff, M.J., Gobetto, R., et al., *Eur. J. Inorg. Chem*., 2013, no. 13, p. 2447.
24. Mayberry, D.D., Nesterov, V.N., and Richmond, M.G., *Organometallics*, 2019, vol. 38, p. 2472.
25. Sokolov, M.N., Fedin, V.P., and Sykes, A.G., *Comprehensive Coordination Chemistry II*, 2003, vol. 4, p. 761.
26. Gushchin, A.L., Hernandez-Molina, R., Anyushin, A.V., et al., *New J. Chem.*, 2016, vol. 40, no. 9, p. 7612.
27. Pino-Chamorro, J.A., Gushchin, A.L., Fernández-Trujillo, M.J., et al., *Chem.-Eur. J.*, 2015, vol. 21, no. 7, p. 2835.
28. Morant-Giner, M., Brotons-Alcázar, I., Shmelev, N.Y., et al., *Chem.-Eur. J.*, 2020.
29. Gushchin, A.L., Laricheva, Y.A., Sokolov, M.N., et al., *Russ. Chem. Rev.*, 2018, vol. 87, no. 7, p. 670.
30. Hernandez-Molina, R., Gushchin, A., González-Platas, J., et al., *Dalton Trans.*, 2013, vol. 42, no. 42, p. 15016.
31. Fedorov, V.E., Mironov, Y.V., Naumov, N.G., et al., *Russ. Chem. Rev.*, 2007, vol. 76, no. 6, p. 529.
32. Bustelo, E., Gushchin, A.L., Fernández-Trujillo, M.J., et al., *Chem.-Eur. J.*, 2015, vol. 21, no. 42, p. 14823.
33. Sokolov, M.N., Gushchin, A.L., Abramov, P.A., et al., *Inorg. Chem.*, 2007, vol. 46, no. 11, p. 4677.
34. Sokolov, M.N., Gushchin, A.L., Naumov, D.Y., et al., *Inorg. Chem.*, 2005, vol. 44, no. 7, p. 2431.
35. Gushchin, A.L., Llusar, R., Vicent, C., et al., *Eur. J. Inorg. Chem.*, 2013, vol. 2013, no. 14, p. 2615.
36. Recatalá, D., Llusar, R., Gushchin, A.L., et al., *ChemSusChem*, 2015, vol. 8, no. 1, p. 148.
37. Laricheva, Y.A., Gushchin, A.L., Abramov, P.A., et al., *Polyhedron*, 2018, vol. 154, p. 202.
38. Pino-Chamorro, J.Á., Laricheva, Y.A., Guillamón, E., et al., *Inorg. Chem.*, 2016, vol. 55, no. 19, p. 9912.
39. Pino-Chamorro, J.A., Laricheva, Y.A., Guillamón, E., et al., *New J. Chem.*, 2016, vol. 40, no. 9, p. 7872.
40. Gushchin, A.L., Laricheva, Y.A., Abramov, P.A., et al., *Eur. J. Inorg. Chem.*, 2014, vol. 2014, no. 25, p. 4093.
41. Pedrajas, E., Sorribes, I., Gushchin, A.L., et al., *ChemCatChem*, 2017, vol. 9, no. 6, p. 1128.
42. Gushchin, A.L., Laricheva, Y.A., Piryazev, D.A., et al., *Russ. J. Coord. Chem*., 2014, vol. 40, no. 1, p. 5. https://doi.org/10.1134/S1070328414010023
43. Kryuchkova, N.A., Syrokvashin, M.M., Gushchin, A.L., et al., *Spectrochim. Acta, Part A*, 2018, vol. 190, p. 347.
44. Gushchin, A.L., Sokolov, M.N., Peresypkina, E.V., et al., *Eur. J. Inorg. Chem.*, 2008, vol. 2008, no. 25, p. 3964.
45. Dovydenko, I.S., Laricheva, Y.A., Korchagina, K.V., et al., *J. Phys. Chem. B*, 2019, vol. 123, no. 41, p. 8829.
46. Pedrajas, E., Sorribes, I., Junge, K., et al., *Green Chem*., 2017, vol. 19, no. 16, p. 3764.
47. Pedrajas, E., Sorribes, I., Junge, K., et al., *ChemCatChem*, 2015, vol. 7, no. 17, p. 2675.
48. Sorribes, I., Wienöfer, G., Vicent, C., et al., *Angew. Chem., Int. Ed. Engl.*, 2012, vol. 51, no. 31, p. 7794.
49. Safont, V.S., Sorribes, I., Andrés, J., et al., *Phys. Chem. Chem. Phys.*, 2019, vol. 21, no. 31, p. 17221.
50. Pino-Chamorro, J.A., Laricheva, Y.A., Guillamón, E., et al., *New J. Chem.*, 2016, vol. 40, no. 9, p. 7872.
51. Gushchin, A.L., Shmelev, N.Y., Malysheva, S.F., et al., *Inorg. Chim. Acta*, 2020, vol. 508, no. 1, p. 119645.
52. Gushchin, A.L., Shmelev, N.Y., Malysheva, S.F., et al., *New J. Chem.*, 2018, vol. 42, no. 21, p. 17708.
53. Laricheva, Y.A., Gushchin, A.L., Abramov, P.A., et al., *J. Struct. Chem*., 2016, vol. 57, no. 5, p. 962.
54. Trofimov, B.A., Gusarova, N.K., Malysheva, S.F., et al., *Synthesis*, 2002, no. 15, p. 2207.
55. *APEX2 (version 1.08), SAINT (version 7.03), SADABS (version 2.11.), SHELXTL (version 6.12)*, Madison: Bruker AXS Inc., 2004.
56. Sheldrick, G.M., *Acta Crrystallog., Sect C: Struct. Chem.*, 2015, vol. 71, p. 3.
57. Dolomanov, O.V., Bourhis, L.J., Gildea, R.J., et al., *J. Appl. Crystallogr.*, 2009, vol. 42, p. 339.
58. Zhou, H., Sun, H., Zheng, T., et al., *Eur. J. Inorg. Chem*, 2015, vol. 2015, no. 19, p. 3139.
59. Rosen, M.S., Spokoyny, A.M., MacHan, C.W., et al., *Inorg. Chem.*, 2011, vol. 50, no. 4, p. 1411.
60. Spokoyny, A.M., Rosen, M.S., Ulmann, P.A., et al., *Inorg. Chem.*, 2010, vol. 49, no. 4, p. 1577.
61. Cunningham, T.J., Elsegood, M.R.J., Kelly, P.F., et al., *Dalton Trans.*, 2010, vol. 39, no. 22, p. 5216.

62. Sokolov, M.N., Gushchin, A.L., Naumov, D.Y., et al., *J. Cluster Sci.*, 2005, vol. 16, no. 3, p. 309.
63. Sokolov, M.N., Gushchin, A.L., Kovalenko, K.A., et al., *Inorg. Chem.*, 2007, vol. 46, no. 6, p. 2115.
64. Beltrán, T.F., Pino-Chamorro, J.Á., Fernández-Trujillo, M.J., et al., *Inorg. Chem.*, 2015, vol. 54, no. 2, p. 607.
65. Alfonso, C., Feliz, M., Safont, V.S., et al., *Dalton Trans.*, 2016, vol. 45, no. 18, p. 7829.
66. Fedin, V.P., Sokolov, M.N., Virovets, A.V., et al., *Inorg. Chim. Acta*, 1998, vol. 269, no. 2, p. 292.
67. Hernandez-Molina, R., Dybtsev, D.N., Fedin, V.P., et al., *Inorg. Chem.*, 1998, vol. 37, no. 12, p. 2995.
68. Gushchin, A.L., Sokolov, M.N., Naumov, N.Y., et al., *Russ. Chem. Bull.*, 2006, vol. 55, no. 11, p. 1966.
69. Gushchin, A.L., Llusar, R., Vicent, C., et al., *Eur. J. Inorg. Chem.*, 2013, vol. 2013, no. 14, p. 1.
70. Fedin, V.P., Sokolov, M.N., Geras'ko, O.A., et al., *Inorg. Chim. Acta*, 1991, vol. 187, no. 1, p. 2615.
71. Varey, J.E. and Sykes, A.G., *Dalton Trans.*, 1993, vol. 4, no. 22, p. 3293.

Translated by E. Yablonskaya